
Article:
Bondar, D, Basheer, M orcid.org/0000-0002-0835-8029 and Nanukuttan, S (2019) Suitability of alkali activated slag/fly ash (AA-GGBS/FA) concretes for chloride environments: Characterisation based on mix design and compliance testing. Construction and Building Materials, 216. pp. 612-621. ISSN 0950-0618

https://doi.org/10.1016/j.conbuildmat.2019.05.043

Suitability of alkali activated slag/fly ash (AA-GGBS/FA) concretes for chloride environments: Characterisation based on mix design and compliance testing

Dali Bondar[1], Marios Soutsos[1], Muhammed Basheer[2], Sreejith Nanukuttan[1]

[1]School of Natural and Built Environment, Queen's University Belfast, BT9 5AG, UK

[2] School of Civil Engineering, University of Leeds, Leeds, LS2 9 JT, UK

Email: D.Bondar@qub.ac.uk, m.soutsos@qub.ac.uk, p.a.m.basheer@leeds.ac.uk, s.nanukuttan@qub.ac.uk

Abstract

Alkali Activated Materials (AAM's) exhibit superior performance in terms of abrasion and acid resistance and fire protection. Ground granulated blast furnace slag (GGBS) and fly ash are the two most common industrial by-products used as precursors in alkali activated material. Alkali-activated systems based on fly ash often require elevated temperature curing, while GGBS alone can lead to flash setting, low workability and high degree of drying shrinkage. This article presents data from a range of GGBS/fly ash blends designed to avoid elevated temperature curing, with desirable fresh properties. Further the suitability of such blended concrete for their use in chloride environments is outlined with the help of diffusivity testing and binding assessment. The results show that while attractive engineering properties can be achieved, the chloride ingress in the AA-GGBS/FA concretes studied here with ≥ 20% fly ash is moderate to high and this will make them unsuitable for protecting steel reinforced in concrete exposed to chloride environments.

Keywords: alkali activated slag/fly ash (AA-GGBS/FA) concretes, workability, compressive strength, bulk resistivity, chloride diffusion coefficient, chloride binding

1. Introduction

Alkali Activated Materials (AAM's) have been under consideration as an alternative binder system since 1895 [1]. The main limitations facing the commercial adoption of these binders are the challenges in controlling engineering properties when using intrinsically variable waste-derived precursors, and the lack of field performance data, especially in extreme environments. GGBS and fly ash are the major by-products used as precursors for making these types of binders. Previous investigations show that alkali-activated high calcium systems such as AAS concretes usually set rapidly, can have low workability, and sometimes also a high degree of drying shrinkage compared to Portland cement (PC) based systems, and all of these are known to affect durability properties [2-6]. Low calcium alkali activated systems, on the other hand, can exhibit high workability and a lower shrinkage than PC systems [7], but need elevated temperatures for curing and hardening. Chi and Huang [8] studied the behaviour of the binder products and properties of AA-GGBS/FA blended mortars and concluded that better properties, compared to PC, were obtained in terms of compressive strength, flexural strength and water absorption. Abdalqader et al. [9] found that the highest strength of AA-GGBS/FA obtained was with a paste mix consisting of GGBS: fly ash in a 3:1 ratio. Gao et al. reported that concrete with a higher GGBS/fly ash ratio exhibit lower porosity [9-10]. However, despite having been aware of this materials potential for over a century, there is still relatively little known about the durability of AAM's, especially the resistance to chloride ingress and the binding behaviour. It was reported by Roy et al. that the advantageous properties of AA-GGBS/FA are their high early strength, rapid hardening and high ultimate strength, low heat of hydration, and resistance to effects resulting from chemical attack. Diffusion coefficients of $50x10^{-15}$ and $5x10^{-15}$ m^2/s were reported for the blended OPC and GGBS paste activated with NaOH, with 0 and 100% GGBS replacement [11].

In this investigation, blended binder systems were used as they provide control of properties such as setting time, workability, shrinkage, strength and durability compared to those based on 100% fly ash or GGBS. An experimental programme was developed to study the workability, strength development and resistance to chloride ingress for a range of AA-GGBS/FA concrete mixes that do not require high temperature curing. Fresh properties, compressive strength at different ages, bulk resistivity, long term chloride diffusion and binding behaviour were determined and reported for various AA-GGBS/FA concretes.

2. Experimental details

2.1 Materials

The primary raw materials used in this study were GGBS and low-CaO fly ash, which were provided by ECOCEM – Ireland and Power Minerals Ltd, UK, respectively. The chemical and physical properties are presented in Tables 1 and 2. GGBS and fly ash were blended in 80/20, 60/40, 40/60 and 20/80 mass proportions, to be activated and used as binder.

Sodium hydroxide (NaOH) powder or pellets were dissolved in water to produce the alkaline solutions. The chemical composition of the sodium silicate solution was 15.5% sodium oxide (Na_2O), 30.5% silicon oxide (SiO_2) and 54% water. In this study, the percentage Na_2O% in the paste (Na_2O%) was selected to be 6 and 8% by powder (GGBS and fly ash) weight, and the silicate modulus (molar ratio SiO_2/Na_2O) was varied from 0.45, 1.0 and 1.25, by blending sodium silicate and sodium hydroxide.

The aggregates used in this study were crushed basalt from local sources in Northern Ireland and comprised of 16.5 mm and 10 mm crushed coarse aggregates, and 4 mm sand. These were combined in a ratio of 48:12:40 to get the maximum packing density in (AA-GGBS/FA) concrete mixes. The bulk specific gravity and water absorption of these materials were measured based on BS EN 1097-1 and are presented in Table 3. Potable tap water (i.e. drinking water quality) was used to make the concrete mixes.

2.2 Mix details, casting procedure and test specimens

Sixteen (AA-GGBS/FA) concrete mixes were studied with different GGBS/fly ash content, water-to-binder, percentage of alkali and the SiO_2/Na_2O ratio (silica modulus, Ms). The details of the different mixes and their initial properties are presented in Table 4. The total binder content, which is the sum of GGBS, fly ash and solid component of the WG, was kept constant at 425 kg/m^3 for all mixes and the water content in the WG was taken into account while determining the mixing water. For increasing proportions of the fly ash, the W/B for mixtures was reduced while the paste content of the mixtures was kept constant.

Mixing

Blended cements were prepared by dry-mixing GGBS and fly ash in required proportions in a bench top food mixer to get a homogeneous blended powder. Crushed basalt aggregates and sand were dry mixed together in a laboratory pan-mixer for one minute. After adding the blended GGBS and fly ash powder, mixing continued for another 2 minutes. The sodium hydroxide solution was then added, and after 2 minutes of further mixing, sodium silicate solution was added and mixing continued for a further minute. The details of the different mixes and their essential properties are presented in Table 4.

Casting and curing of the specimens

Fresh properties of concrete were measured according to BS EN 12350 [12]. From each concrete mix, nine 100 mm cubes, and three 100x200 mm cylinders, were cast for the determination of compressive

strength in accordance with BS EN 12390 [13], bulk resistivity and chloride diffusion coefficient according to Nordtest NT Build 443 [14]. The concrete specimens were cast in three layers and compacted on a vibrating table. After casting, all the specimens (still in the mould) were covered with plastic sheets and left in the casting room for 24 h. They were demoulded and kept in sealed plastic zip bags until the test date. The storage room was maintained at 23ºC & 65% RH.

2.3 Testing procedures

Chloride transport through AA-GGBS/FA concretes was assessed using a non-steady state chloride diffusion test, Nordtest NT Build 443 [14]. One day before the test age of 91 days, the 100x200 mm concrete cylinders were cut to four slices of diameter 100 mm with a thickness of 50 mm per mix. A slice with a thickness of 50 mm from the cast surface (trowel finished face) was considered for measuring bulk resistivity, and the rest were kept for carrying out the chloride diffusion test. The vacuum saturation regime specified in the standard was used to precondition the slices so that the chloride flow is predominantly diffusive, and initial sorption or capillary forces are negligible. The vacuum was applied to remove air for three hours and released afterwards. Samples were wrapped in hessian saturated in deionised water to prevent leaching of ions, and placed in the container. The weight of the sample was noted after an hour (W_1) and then vacuum was applied, followed by further saturation. Weight was checked again (W_2). Usually after 6 hours, when W_i-$W_{(i-1)}$ was less than 0.1%, the samples were considered fully saturated; if not, saturation was continued until this criterion was met. After conditioning to a surface-dry condition, an epoxy resin was applied onto the surfaces of the specimens in three layers except the exposure face (saw cut face). When the epoxy coating was dry, the cores were immersed in a NaCl solution of concentration 165 g/L (~2.82 M) for six months. After immersion, two cores for each mix were profile ground to obtain concrete dust from different depths up to a depth was determined for each sample by spraying a 0.1 N AgNO3 solution on the third freshly broken concrete sample. These depths were measured from the exposed surface. The total chloride content of the dust samples was determined in accordance with the recommendations of RILEM TC 178-TMC [15] using a pre-calibrated potentiometric titration method. The concrete dust was dissolved in deionised water in accordance with RILEM TC 178-TMC recommendations, considering 3-5 min digestion [16] to measure the pH value of the suspension, and for the determination of water soluble chlorides. Chloride diffusivity and the surface chloride content were determined by using curve fitting to the error function solution of Fick's second law of diffusion, as described in NT BUILD 443 [14].

3. Results and discussions

The following sections discuss the slump, flow and air content, compressive strength, chloride diffusivity, and chloride binding capacity of AA-GGBS/FA concretes. The histograms categorize the results for groups of concretes with different ratios of GGBS/FA and the contours graph are a good map for designing AA-GGBS/FA concretes mixes based on GGBS/FA ratio and activator parameters (Na_2O%*Ms).

3.1 Slump, flow and air content

The purpose of this testing programme was to demonstrate the range of slump values that AA-GGBS/FA concretes is capable of producing, and the changes to the governing variables that are necessary to achieve high slump with low air content of the GGBS/FA mixes to have better mixes for durability. The slump and flow results of the concretes are presented in Figures 1 and 2. The slump values of the concretes show that all the mixes had a slump value greater than 120 mm. It can be observed that although W/B was adjusted based on the proportion of the fly ash in the system, increasing the fly ash in the blend increased the workability, and the maximum workability was achieved for mix with the maximum fly ash content due to its bubble structure which increase the lubricity. The literature shows that increasing the sodium oxide content results in increased

workability, reduced setting times and higher compressive strength. However, high concentrations resulted in loose structure in sodium hydroxide activated samples because of the excess water is being retained in the system before forming a monolithic hydrated structure [18, 19]. For mixes with the same GGBS to fly ash content and water to binder ratios, comparing mixes 1, 5, 9 and 13 and mixes 4, 8, 12 and 16 respectively, the slump values of the AA-GGBS/FA concretes with the same Ms ratio increased with an increase of Na_2O%. The slump values also increased with the increase of Ms which can be seen by comparing odd and even mixes (e.g. mix no. 1 against 2, 3 against 4) in the two groups with two different Na_2O% and the same ratios of GGBS to fly ash.

As is evident from Fig. 1, the AA-GGBS/FA concretes can be designed for S3, S4 and S5 slump ranges. Thus, all the mixes meeting the minimum slump requirement for their use in chloride environments, such as S2 specified in BS8500-1:2015 for different exposure of marine environments [17].

The contour map graphs in Figure 3 (a) and (b) shows the results of slump and flow test against GGBS/FA ratio and a function of activator parameters or (Na_2O%*Ms) values for different mixes with same paste content. (Na_2O%*Ms) is the ratio of the SiO_2 content of the activator to the total cementitious materials content for mixes. It is depicted from both figures that increasing the GGBS/FA ratio, decreases the workability of mixes for GGBS/FA<0.67 and GGBS/FA>1.5 while increases that for 0.67<GGBS/FA<1.5. The maximum workability of mixes happens when 1.5<GGBS/FA<2.5 when (Na_2O%*Ms) values is less than 7.5. It is also evident from these figures that workability increased when (Na_2O%*Ms) was increased which can be due to disparity of silica in solution form.

The air content of the GGBS/FA mixes are presented in Figure 4 and Figure 5 and they show the contour graph for air content in fresh mixes of AA-GGBS/FA concretes against GGBS/FA ratio and (Na_2O%*Ms) values. The lowest air content was measured for mixes with a GGBS/fly ash ratio of 60/40 while the highest was for 20/80 (except mix 15) while considering the map analysis there is two ideal island which shows the minimum air content in the fresh AA-GGBS/FA concretes. These two islands happen when 0.6<GGBS/FA<1.0 or 1.0<GGBS/FA<2.25 and the (Na_2O%*Ms) for mixes is more than 6.75% and less than 4.25%, respectively which are recommendable to have workable AA-GGBS/FA concrete with low air content. Figure 4 also shows in the mixes made with a higher alkali percentage, the air content is lower (comparing Mixes 1, 5 and 13 to Mixes 4, 8 and 16, respectively) and higher Ms for mixes has had no major effect, especially for mixes with higher alkaline content (comparing Mixes 3 to 4 or 7 to 8). However higher silica content in the activator was more effective when the fly ash proportion increased in the blend, and this causes higher air content when using higher silica content (comparing Mixes 15 to 16) which means silica do not let air to be pushed out from fresh concrete.

3.2 Compressive strength

Figure 6 shows the compressive strengths of AA-GGBS/FA concrete mixes at 2, 28 and 90 days. From the results, it can be stated that: (1) the first three groups had more than 20 MPa after 2 days and more than 50 MPa after 28 days curing and 28 day strength is 80–90% of the 91 day strength, offering insight into the short and long term microstructural development in such binders, (2) as is expected, the more fly ash in the system, the lower is the early age and long term strength, (3) an increase in Na_2O% and Ms generally increases the compressive strength of AA-GGBS/FA concretes, which agrees with the results reported by others. The last one is due to more N-A-S-H (sodium alumina silicate hydrate) reaction product being generated, based on the increase of Na_2O%, and more C-A-S-H (calcium alumina silicate hydrate) reaction product being produced, based on the increase of SiO_2 content. Silica modulus of 0.45 will drop down the strength for Na_2O% of 8% and this can be because of low silica content in the activator to make the gel formation. The activated GGBS/fly ash concretes with Ms of 1.0 up to 1.25 generally obtained the highest compressive strength (see Figure 6), which

also has a good agreement with the literature and shows that the activated GGBS/fly ash with Ms of around 1.0 obtains the best hydration. From the 28day compressive strengths, Table 4 and Figure 6 both show that except mixes no. 7(1.5-8%-0.45), 11(0.67-8%-0.45) and 13 to 16 with GGBS/FA=0.25, all achieved the required strength for the EN206 exposure classes XS3 and XD3 which is equivalent to an average strength ≥ 56.99 MPa (calculated as 45 +1.48(8.1) MPa; where 8.1 is the standard deviation of the test results). However, mixes 7(1.5-8%-0.45), 11(0.67-8%-0.45) and 16(0.25-8%-1.0) met the strength requirement of 48.99 (=37+1.48(8.1)) MPa for the exposure classes XS1, XD1 and XD2. Although it was evident that the strength requirement and w/b will not comply with BS 8500-1:2015 norms, the intention of including the mixes were to assess their performance against Cl^- ingress.

Figure 7 (a) to 7 (c) presents the contour map of 2, 28 and 90 days compressive strength against GGBS/FA ratio and (Na_2O%*Ms) values. In general, there is an increase in the 2, 28-days compressive strength values with increase in the SiO_2 content of the activator to the total cementitious materials content. However, when the SiO_2 content of the activator reach to 6.5% and 7.5% of the total cementitious materials content respectively the reverse trend is started. 90-days compressive strength does not change significantly for GGBS/FA ratio >1.5 and (Na_2O%*Ms) >6.

3.3 Bulk electrical resistivity

Electrical resistivity can evaluate microstructure of concrete and be related to the pore structure and conductivity of the pore solution to predict the diffusion coefficients of chloride ions. The test set-up for measuring bulk resistivity is shown in Figure 8. Figure 9 depicts the average bulk electrical resistivity for different AA-GGBS/FA concrete mixes. Higher resistivity could be attributed to denser structure with low connected porosity and/or less conductivity of the binder matrix and such mixes will be expected to be superior in resisting ionic (chloride) flow. Higher GGBS content in AA-GGBS/FA concretes resulted in higher bulk resistivity, while mixes with higher alkali content show higher bulk resistivity when GGBS dominates the blend. Furthermore, bulk electrical resistivity decreases for mixes made with higher silica modulus (except Mixes 3 and 4), whereas the bulk resistivity seems to be a maximum at Na_2O=8% and Ms=1.0 when GGBS/FA=80/20. This may be related to the alkali content which is required to produce maximum reaction products and gives the confidence for designing the concretes for strength and durability.

Figure 10 shows contour graph of bulk electrical resistivity for different mixes against GGBS/FA ratio and (Na_2O%*Ms) values. It is depicted from Figure 10 that for mixes with GGBS/FA < 0.67 the SiO_2 content of the activator has minimal influence on bulk resistivity and the resistivity does not change for (Na_2O%*Ms) < 6.25%. This can show that for GGBS to fly ash less than 0.67 and (Na_2O%*Ms) < 6.25% pore structure dominates the conductivity of the system which is not dependent to the activator specification. Whereas for (Na_2O%*Ms) > 6.25% the resistivity decreases with increasing of the (Na_2O%*Ms) which shows that pore solution domination and higher conductivity because of free ions in the binder matrix reduce the resistivity. For mixes with same (Na_2O%*Ms) the bulk resistivity increases with increasing of GGBS to fly ash ratio for GGBS/FA <0.67 and GGBS/FA >1.5. This shows the effect having denser structure and is because of higher GGBS content in the binder matrix of mixes. While for 0.67<GGBS/FA <1.5 and (Na_2O%*Ms) <7.5 pore solution domination causes the reduction of resistivity and higher conductivity because of free ions in the pore solution. This can show the range of (Na_2O%*Ms) which is suitable for activation corresponding to different GGBS to fly ash ratio and should be more than 7.5 for 0.67<GGBS/FA<1.5.

3.5 Chloride diffusion

Concrete sample disks with all surface painted except the top face, placed in air tight container with sodium chloride solution for diffusion test as per NT Build 443 are shown in Figure 11.

Figure 12 presents average chloride diffusion depth and D_{nssd} for mixes. As shown in Figure 12 the chloride diffusion depth of AA-GGBS/FA concretes was from 13 mm for mixes 2(6%-1.25), 3(8%-0.45), 4(8%-1.0) with GGBS/FA=80/20 to 40 mm for mixes 13(6%-1.0) and 14(6%-1.25) with GGBS/FA=20/80.

The non-steady state diffusion coefficient with AA-GGBS/FA concretes was resulted between $1.05*10^{-12}m^2/s$ [mix3 (8%-0.45)] with GGBS/FA=80/20 and $126.51*10^{-12}m^2/s$ [mix14 (6%-1.25)] with GGBS/FA=20/80. It can be seen that all the D_{nssd} for AA-GGBS/FA concretes was moderate to high except for the mixes with GGBS to fly ash ratio of 80/20. This is in line with Mundra et al. findings that states for fly ash blended AAMs concretes service life influenced by Cl^- transport. The non-steady diffusion coefficient, D_{nssd}, of the AA-GGBS/FA concretes was found to be influenced by the fly ash content, Na_2O% and Ms (at mixes with low alkali content). All the D_{nssd} values for AA-GGBS/FA concretes were higher for higher fly ash content which is due to the influence of larger pore size and more pore connectivity of the concrete.

The third group of data, with average X_d closer to 35 mm, the average D_{nssd} is 13.56. This is three times bigger than second group which has an X_d close to 30. This can be because of more chloride absorption in third group which has more fly ash in the system. Activated fly ash has been stated to have zeolite formation with better initial surface absorption (physical chloride binding) than activated slag [21]. Surface absorption is stated the main responsible for around 90% of the total chloride uptake [22].

Figure 13 shows the contour map of D_{nssd} of different AA-GGBS/FA concrete mixes against GGBS/FA ratio and (Na_2O%*Ms) values. D_{nssd} of AA-GGBS/FA concrete mixes does not change significantly with increase of the ratio of the SiO_2 content of the activator to the total cementitious materials content for GGBS/FA ratio <1.0 and (Na_2O%*Ms) <6.0. Furthermore (Na_2O%*Ms) =6.0 is an extreme point and at which D_{nssd} of AA-GGBS/FA concrete mixes for values less than 6.0 is decreasing while for values more than 6.0 is increasing. The plaid area in Figure 13 shows the limits of designing AA-GGBS/FA concrete mixes suitable for chloride exposure environments, if reinforcing steel is preferred.

3.4 Chloride binding in AA-GGBS/FA concrete

There is limited information available on chloride binding of AA-GGBS/FA concrete in the literature. The available CSH and aluminate phases (C-(N)-A-S-H or two layered double hydroxides) in activated GGBS contribute to the physical and chemical binding reactions [22, 23] while there is no information on the conformed phases in activated fly ash systems to show contribution of that to chloride binding reactions. Binding behavior of different alkali activated slag (AAS) concrete was reported in previous article by the authors [24]. Following the same procedure, the total and water-soluble chloride concentration of the concrete dust removed for chloride diffusion test in section 3.3 were determined for mixes 13-16. This data is presented in Figures 14 a-d along with the corresponding pH values. It is evident from Figure 14 that for the mixes studied, the total chloride concentration is almost entirely represented by water-soluble chlorides. It is known that pH reduction can release the Cl^- otherwise bound to Friedel's salt [25] in PC based systems. In a typical PC based system, the total Cl^- will be composed of both bound and free chlorides, and free chloride is often represented by the water-soluble fraction which may also contain a proportion of the adhered Cl^- physically bound to the cement phases. Two aspects are noticeable from the figure, (1) the pH values are $\leq$ 11 for most depth (or all depth), (2) the surface region is undergoing leaching-induced changes during Cl^- transport that result in a reduction of pH; there is also a skin effect which causes a near-surface dip in the total Cl^- content. While as resulted in previous study, for alkali activated slag (AAS) concrete the pH values are >11 for most depth and the surface region occurs within the depth of 5-12 mm [24].

The main reaction product in AA-GGBS/FA concrete is a Na-Al silicate hydrate (N-A-S-H) gel which it seems have no tendency to bind chlorides in the alkalinity range observed in mixes 13-16. The lower alkalinity could have affected the stability of the reaction products that bind chlorides. The least fluctuation in pH reduction is for the mix 13, that has 6% Na_2O and Ms = 1.

The results presented in this article shows that AA-GGBS/FA with GGBS/FA ratio less than 2.5 are not suitable for chloride exposure environments, if reinforcing steel is preferred. If the GGBS/FA ratio is between 2.5 and 4, silica content in the activators should be selected based on Figure 13 to have concrete with low diffusivity.

4. Conclusion

1. Results show that it is possible to achieve desirable fresh properties and compressive strength for AA-GGBS/FA concrete when cured at 20^0C. This means such concretes do not require elevated temperature curing for strength gain.
2. A higher proportion of GGBS results in high early and long-term strength.
3. AA-GGBS/FA concretes with GGBS to fly ash ratio less than 4 have moderate to high chloride migration coefficients, making them non-viable for protection of reinforcing steel in chloride environments.
4. The blends can be categorised based on the GGBS to fly ash ratio (GGBS/FA) as low diffusivity (GGBS/FA = 80/20), high diffusivity (GGBS/FA = 60/20), and very high diffusivity (GGBS/FA = 40/60 & 20/80).
5. No bound chloride in the alumina silicate-dominated alkali-activated concretes, characteristic of a lack chemical binding in the fly ash dominated AA-GGBS/FA concretes and as a result, the chloride diffusivity in these binders depends on the role of the pore structure in physical chloride binding and encapsulation which highlights the importance of the pore structure studies in AA-GGBS/FA concretes.
6. Typically, workable AA-GGBS/FA concretes require binder content of 425 kg/m^3 (GGBS/FA=4) and a water/binder of 0.47, which is close to the maximum acceptable limit for XD3 and XS3 chloride exposure classes as per BS 8500.

Acknowledgements

The authors gratefully acknowledge the Engineering and Physical Sciences Research Council for providing the financial support for conducting this work [EP/M003272/1]. The authors would like to acknowledge the technical support provided by Dr. John Provis at The University of Sheffield as PI of the project.

References

[1] J. Whiting, ‘‘Manufacture of Cement”, U.S. Patent 544,706, 1895.

[2] A. M. Rashad, Properties of alkali-activated fly ash concrete blend with slag, Iran Journal of Material Science and Engineering, 10 (1), 2013, 57-64

[3] S. Aydin, A ternary optimization of mineral additives of alkali activated cement mortars, Constr. Build. Mater. 43 (2013) 131-138

[4] N.K. Lee, H.K. Lee, Setting and mechanical properties of alkali-activated fly ash/slag concrete manufactured at room temperature, Constr. Build. Mater. 47 (2013) 1201-1209

[5] F. Collins, J. Sanjayan, Effect of pore size distribution on drying shrinkage of alkali activated slag concrete, Cem. Concr. Res., 30 (2000) 1401-1406

[6] A.A. Melo Neto, M.A. Cincotto, W. Repette, Drying and autogenous shrinkage of pastes and mortarwith activated slag cement, Cem. Concr. Res., 38 (2008) 565-574

[7] Y. Ma, G. Ye, The shrinkage of alkali activated fly ash, Cem.Concr. Res., 368 (2015) 75-82

[8] M. Chi, R. Huang, "Binding mechanism and properties of alkali-activated fly ash/slag mortars", Constr. and Build. Mater. 40 (2013) 291–298

[9] A.F. Abdalqader, F. Jin, A. Al-Tabbaa, Characterisation of reactive magnesia and sodium carbonate-activated fly ash/slag paste blends, Constr.Build. Mater. 93 (2015) 506–513

[10] X. Gao, Q.L. Yu, H.J.H. Brouwers, Assessing the porosity and shrinkage of alkali activated slag-fly ash composites designed applying a packing model, Constr. Build. Mater. 119 (2016)175-184

[11] D. M. Roy, W. Jiang, M.R. Silsbee, Chloride diffusion in ordinary, blended, and alkali-activated cement pastes and its relation to other properties, Cem. Concr. Res. 30 (2000) 1879-1884

[12] BS EN 12350-2, 5&7, Testing fresh concrete-Part 2, 5&7: Slump test and Flow test and Air content measurement, BSI, London, 2009

[13] BS EN 12390-3, Testing hardened concrete-Part 3: Compressive strength of test specimens, BSI, London, 2009

[14] NT BUILD 443, Concrete, hardened: accelerated chloride penetration, NORDTEST, Espoo, 1995

[15] RILEM TC 178-TMC: Testing and modelling chloride penetration in concrete. Analysis of total chloride content in concrete, recommendation, Mater. Struct. 35 (2002) 583-585

[16] RILEM TC 178-TMC: Testing and modelling chloride penetration in concrete. Analysis of water soluble chloride content in concrete, recommendation, Mater. Struct. 35 (2002) 586-588

[17] BS 8500-1, Concrete—complementary British Standard to BS EN 206-1—part 1: method of specifying and guidance for the specifier, BSI, London, 2015

[18] D. Bondar, C.J. Lynsdale, N.B. Milestone, N. Hassani, A.A. Ramezanianpour, Effect of type, form, and dosage of activators on strength of alkali-activated natural pozzolans, Cem. Concr. Compos. 33 (2011) 251–260

[19] D. Bondar, S. Nanukuttan, M. Soutsos, P.A. Muhammed Basheer, J. Provis, Suitability of alkali activated GGBS/Fly ash concrete for chloride environments. in Tagnit-Hamou, A.(eds), The 10th ACI/RILEM International Conference on Cementitious Materials and Alternative Binders for Sustainable Concrete, 2-4 October 2017, Montreal, Canada, 2017, 35.1-35.14

[20] S. Mundra, S.A. Bernal, M. Criado, P. Hlaváček, G. Ebell, S. Reinemann, G.J.G. Gluth, J.L. Provis, Steel corrosion in reinforced alkali-activated materials, RILEM Technical Letters, 2 (2017) 33-39

[21] M.W. Grutzeck, S.Kwan, M. DiCola, Zeolite formation in alkali-activated cementitious systems, Cem. Concr. Res. 34(6) (2004) 949-955 ·

[22] X. Ke, S.A. Bernal, J.L. Provis, Uptake of chloride and carbonate by Mg-Al and Ca-Al layered double hydroxides in simulated pore solutions of alkali activated slag cement, Cem. Concr. Res. 100 (2017) 1–13.

[23] X. Ke, S.A. Bernal, O.H. Hussein, J.L. Provis, Chloride binding and mobility in sodium carbonate-activated slag pastes and mortars, Mater. Struct. 50 (2017) #252.

[24] D. Bondar, Q. Ma, M. Soutsos, M. Basheer, J.L. Provis, S. Nanukuttan, Alkali activated slag concretes designed for a desired slump, strength and chloride diffusivity, Constr. Build. Mater. 190 (2018) 191–199

[25] M. Castellote, C. Andrade, C. Alonso, Chloride-binding isotherms in concrete submitted to non-steady-state migration experiments, Cem. Concr. Res., 29 (1999) 1799-1806

393 Table 1: Oxide composition of GGBS & Fly ash

precursor	Component (mass% as oxide)						
	SiO_2	Al_2O_3	CaO	Fe_2O_3	MgO	others	LOI
GGBS	35.7	11.2	43.9	0.3	6.5	2.09	0.31
Fly ash	46.8	22.5	2.2	9.1	1.3	14.5	3.6

394

395 Table 2**:** Physical properties of GGBS & Fly ash

Material	GGBS	Fly ash
Fineness ≥45 μm	7.74%	18.39%
Particle density	2.86	2.21
Water absorption	35.14%	27%

396

397 Table 3**:** Physical properties of aggregates

Aggregates	Bulk specific gravity	Bulk SSD Specific gravity	Water Absorption (%)
Sand (0-4mm)	2.72	2.73	0.75
Fine Crushed Agg. (5-10mm)	2.67	2.75	3.14
Coarse Crushed Agg. (10-16mm)	2.60	2.67	2.60

398

399 Table 4: The details of the different mixes and their properties

Mix No.	GGBS/FA (kg/m^3)	GGBS/FA ratio	Ms (=SiO_2/Na_2O)	Na_2O (%)	W/B	Slump (mm)	2 days Comp. St. (MPa)	28 days Comp. St. (MPa)	Concrete Grades
1	340/85	4	1.0	6	0.47	170	54.6	81.1	C65/80
2	340/85	4	1.25	6	0.47	200	51.2	84.8	C65/80
3	340/85	4	0.45	8	0.47	200	35.2	60.2	C49/60
4	340/85	4	1.0	8	0.47	230	50.9	80.6	C65/80
5	255/170	1.5	1.0	6	0.46	230	42.1	73.4	C56/70
6	255/170	1.5	1.25	6	0.46	240	40.3	78.5	C60/75
7	255/170	1.5	0.45	8	0.46	205	28.8	52.4	C40/50
8	255/170	1.5	1.0	8	0.46	240	31. 9	75.7	C60/75
9	170/255	0.67	1.0	6	0.44	170	28.2	64.8	C49/60
10	170/255	0.67	1.25	6	0.44	210	22.3	69.4	C52/65
11	170/255	0.67	0.45	8	0.44	120	22.2	54.0	C40/50
12	170/255	0.67	1.0	8	0.44	250	23.0	61.2	C49/60
13	85/340	0.25	1.0	6	0.43	225	13.8	42.6	C32/40
14	85/340	0.25	1.25	6	0.43	220	9.5	47.1	C35/45
15	85/340	0.25	0.45	8	0.43	200	9.7	28.4	C20/25
16	85/340	0.25	1.0	8	0.43	250	10.4	49.2	C35/45

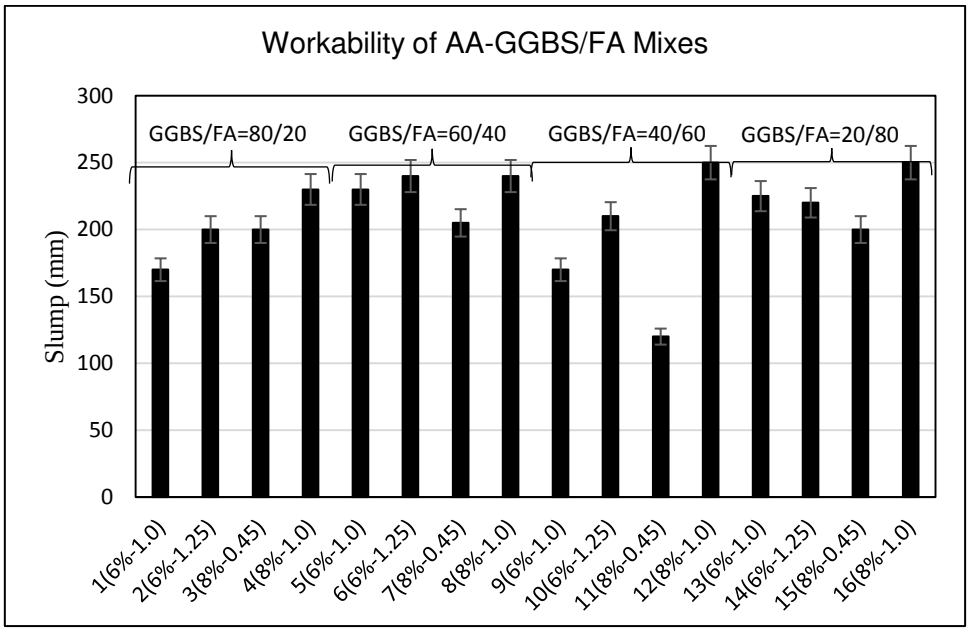

Fig. 1-Slump results of AA-GGBS/FA concretes

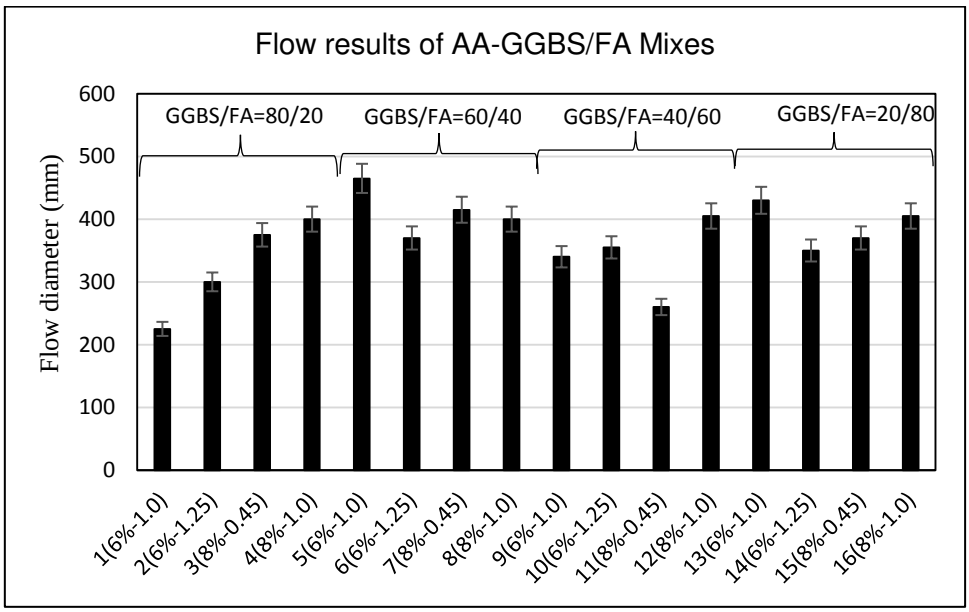

Fig. 2-Flow results of AA-GGBS/FA concretes

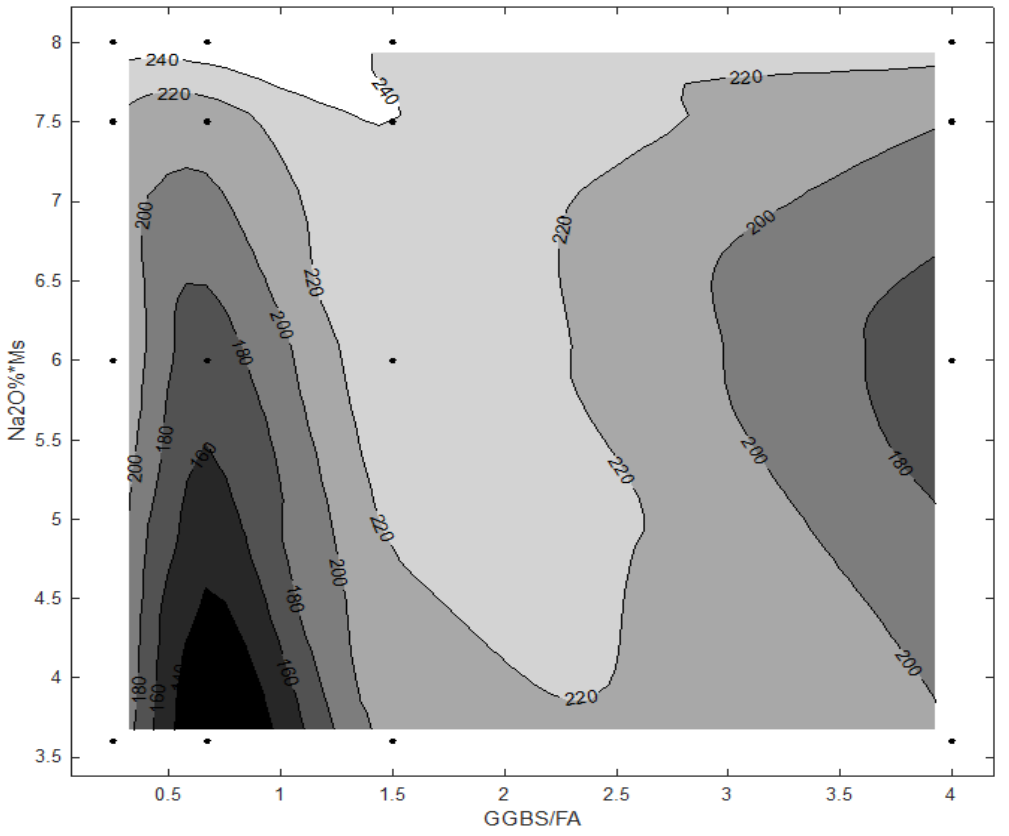

(a)

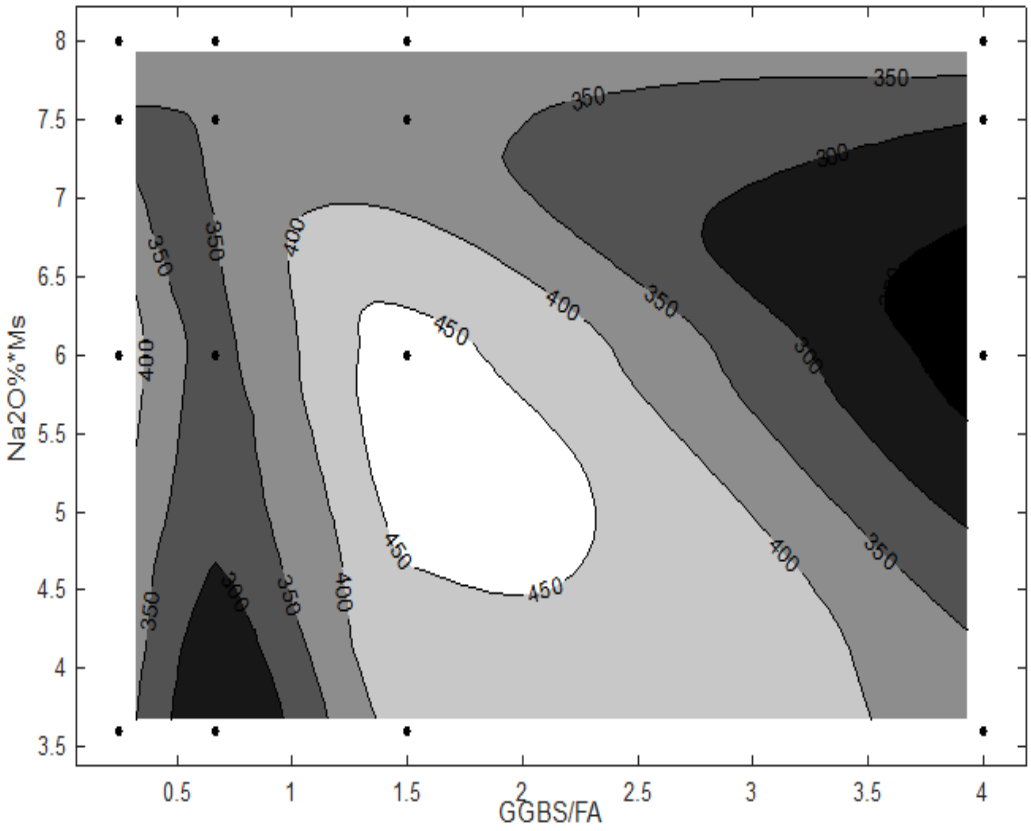

Fig. 3-Contour graph for workability of AA-GGBS/FA concretes - (a) Slump test, (b) Flow test

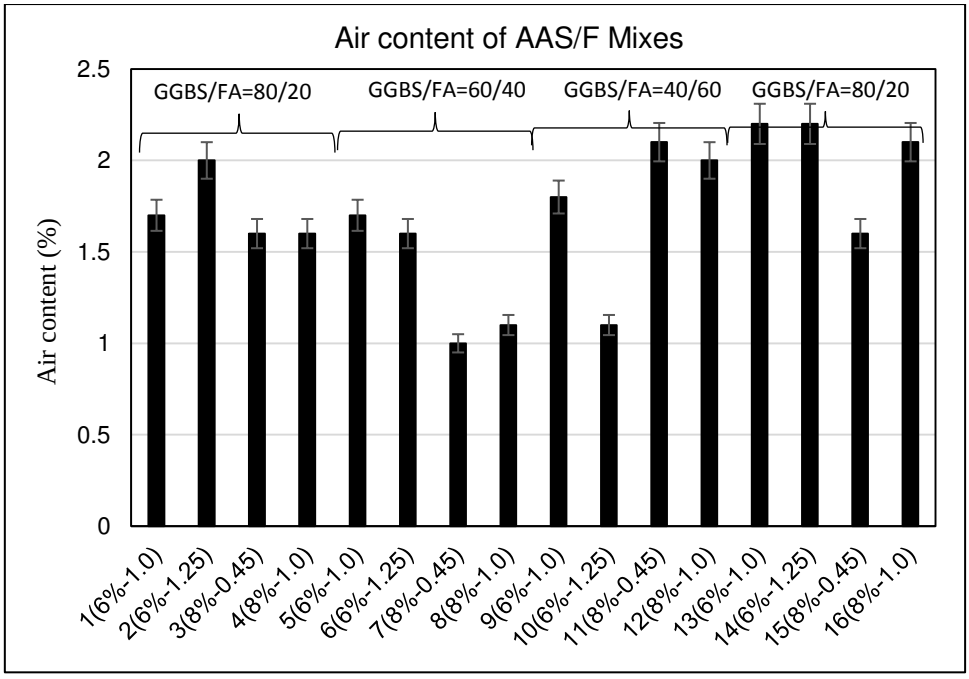

411

412 Fig. 4-Air content in fresh mixes of AA-GGBS/FA concretes

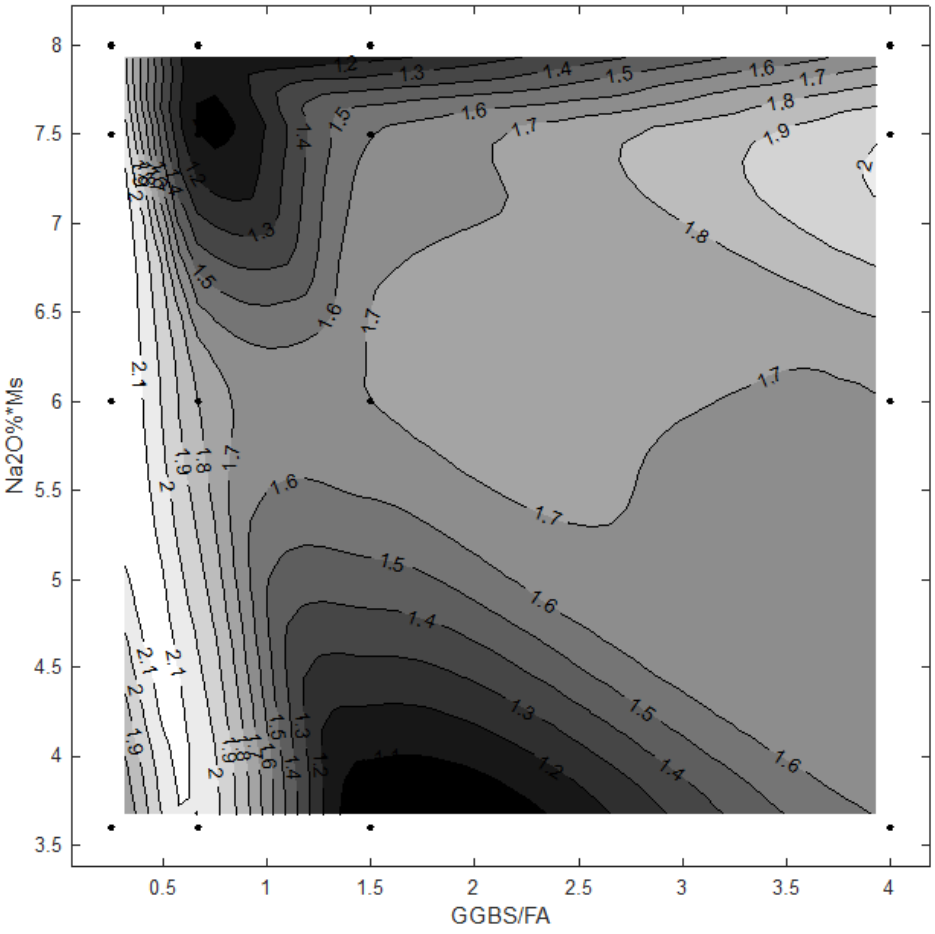

413

414 Fig. 5-Contour graph for air content in fresh mixes of AA-GGBS/FA concretes

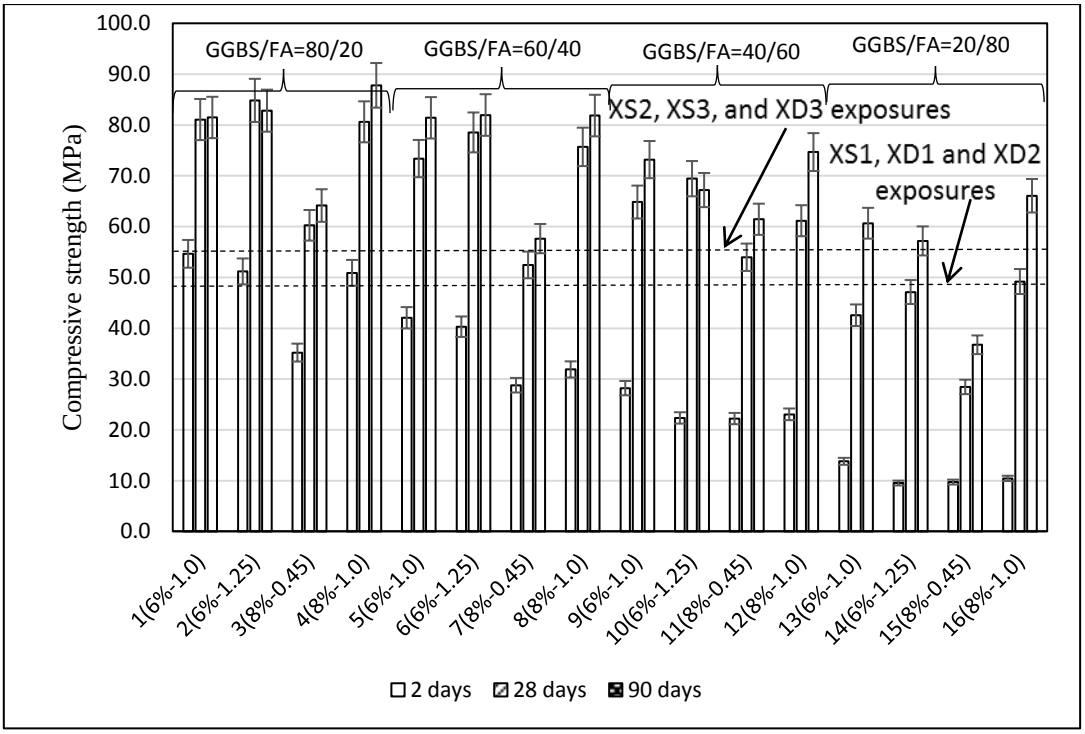

Fig. 6-Compressive strength of AA-GGBS/FA concretes mixes at 2, 28 and 90days

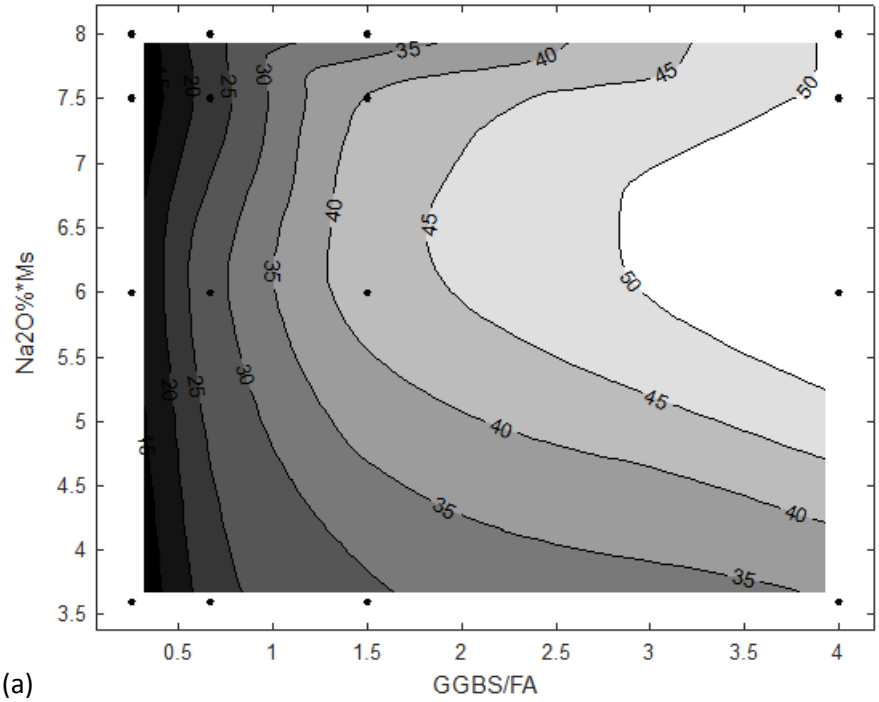

(a)

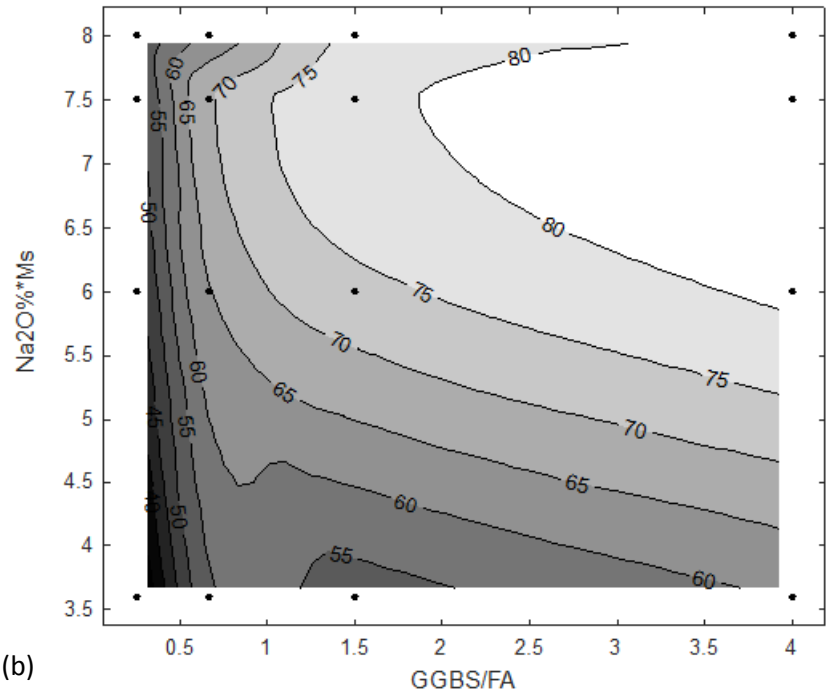

(b)

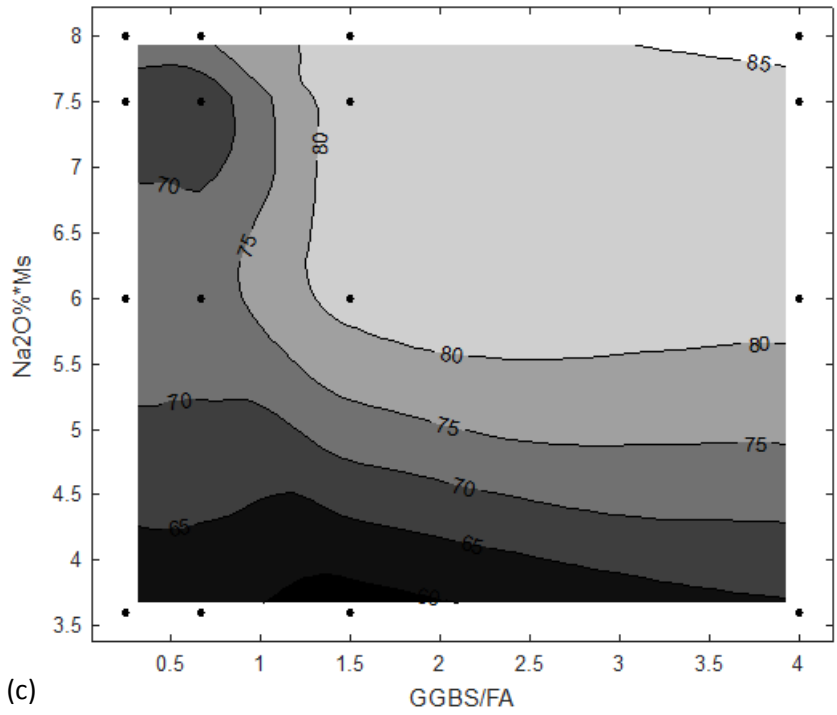

(c)

Fig. 7-Contour graph for compressive strength of AA-GGBS/FA concretes

(a) 2days, (b) 28days, (c) 90days

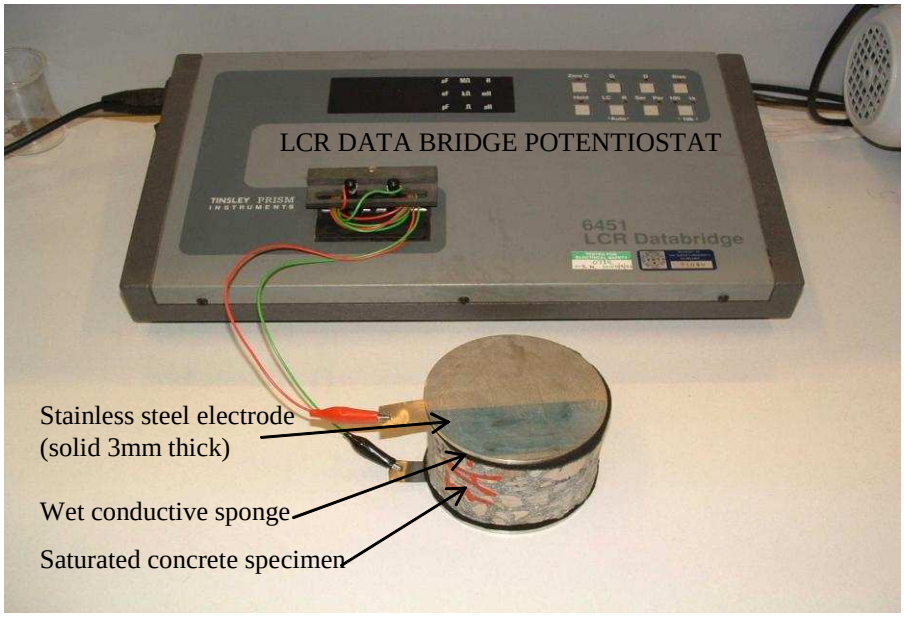

Fig. 8-Bulk resistivity test equipment and sample

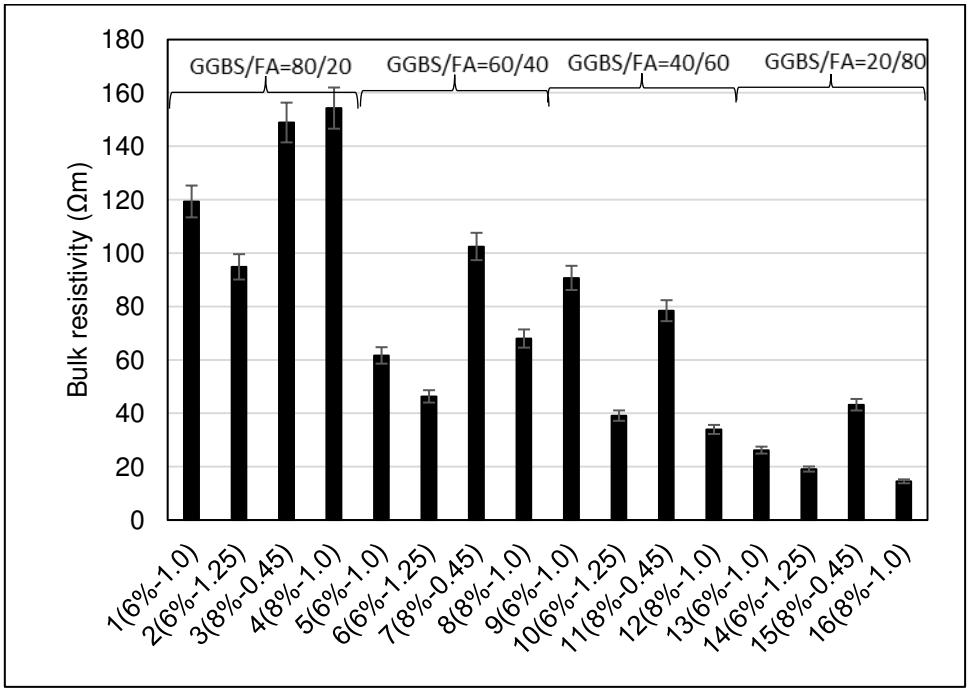

Fig. 9-Bulk resistivity

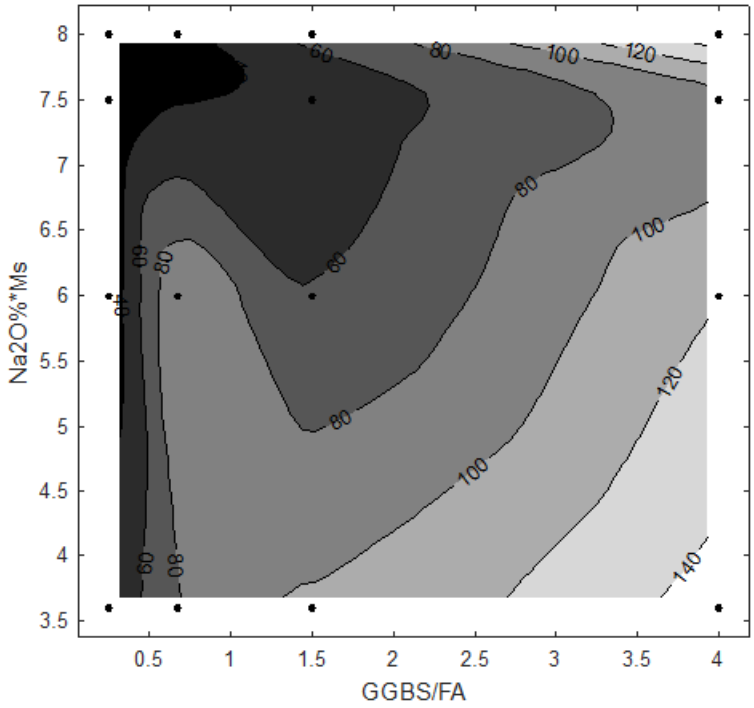

Fig. 10-Contour graph for bulk electrical resistivity (Ω.m) of AA-GGBS/FA concretes

Fig. 11-Concrete sample disks with all surface painted except the top face, placed in air tight container with sodium chloride solution for diffusion test as per NT Build 443

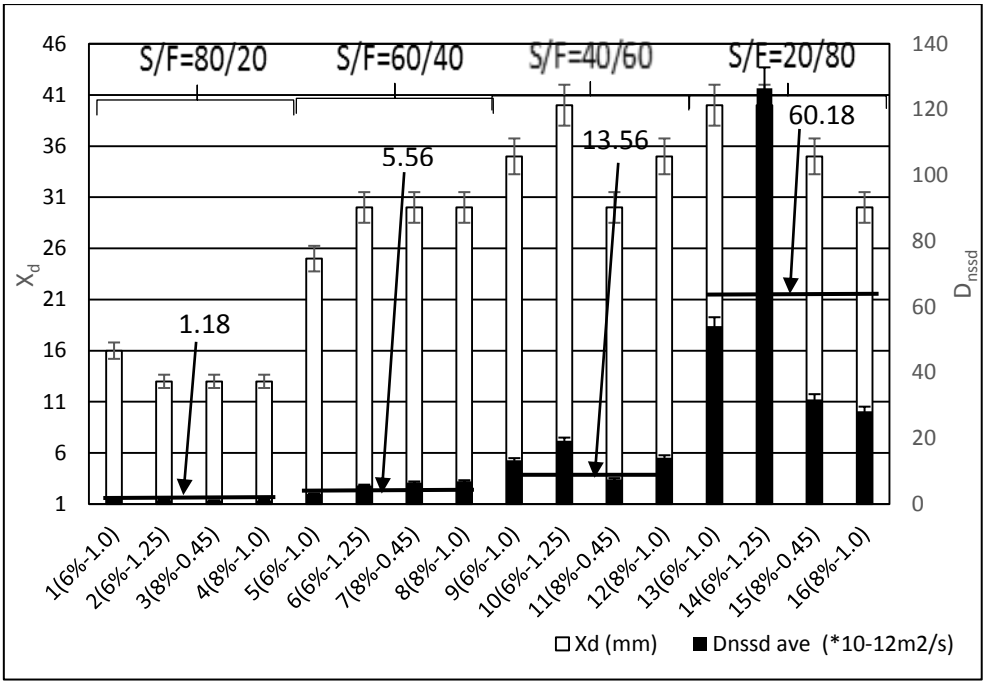

Fig. 12-Chloride penetration depths (X_d) and D_{nssd} of AA-GGBS/FA concretes

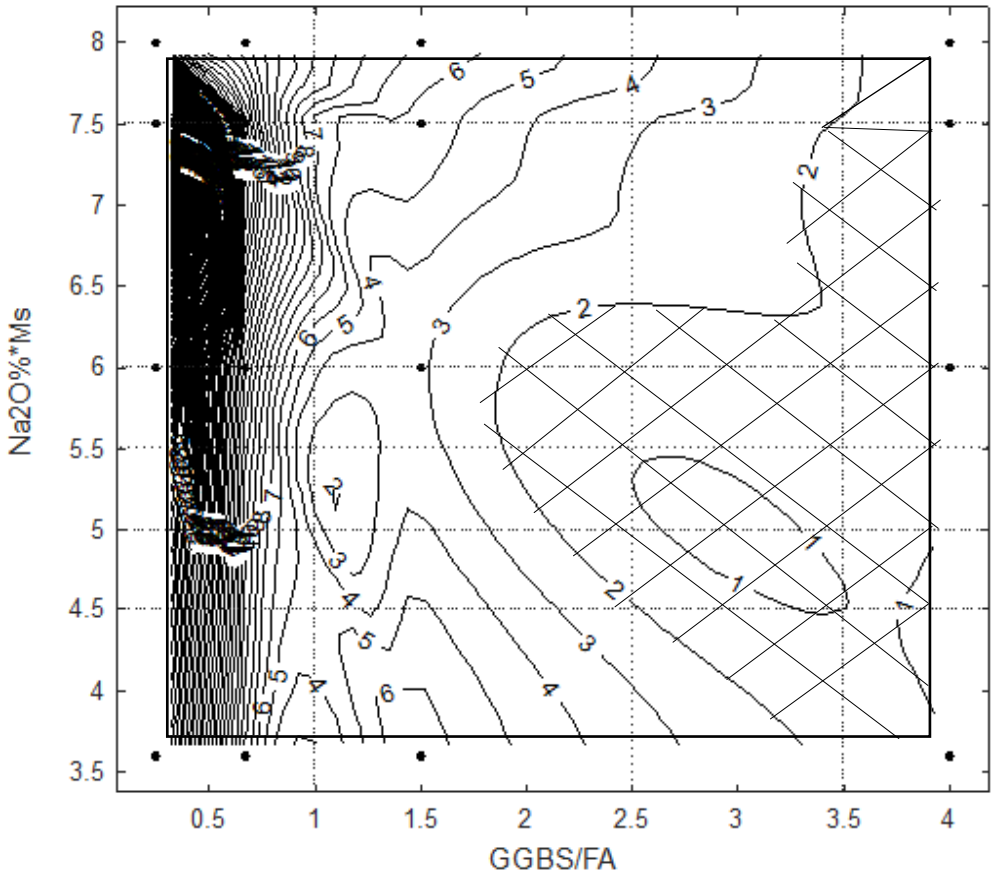

Fig. 13-Contour graph for D_{nssd} ($x10^{-12}$ m^2/s) of AA-GGBS/FA concretes

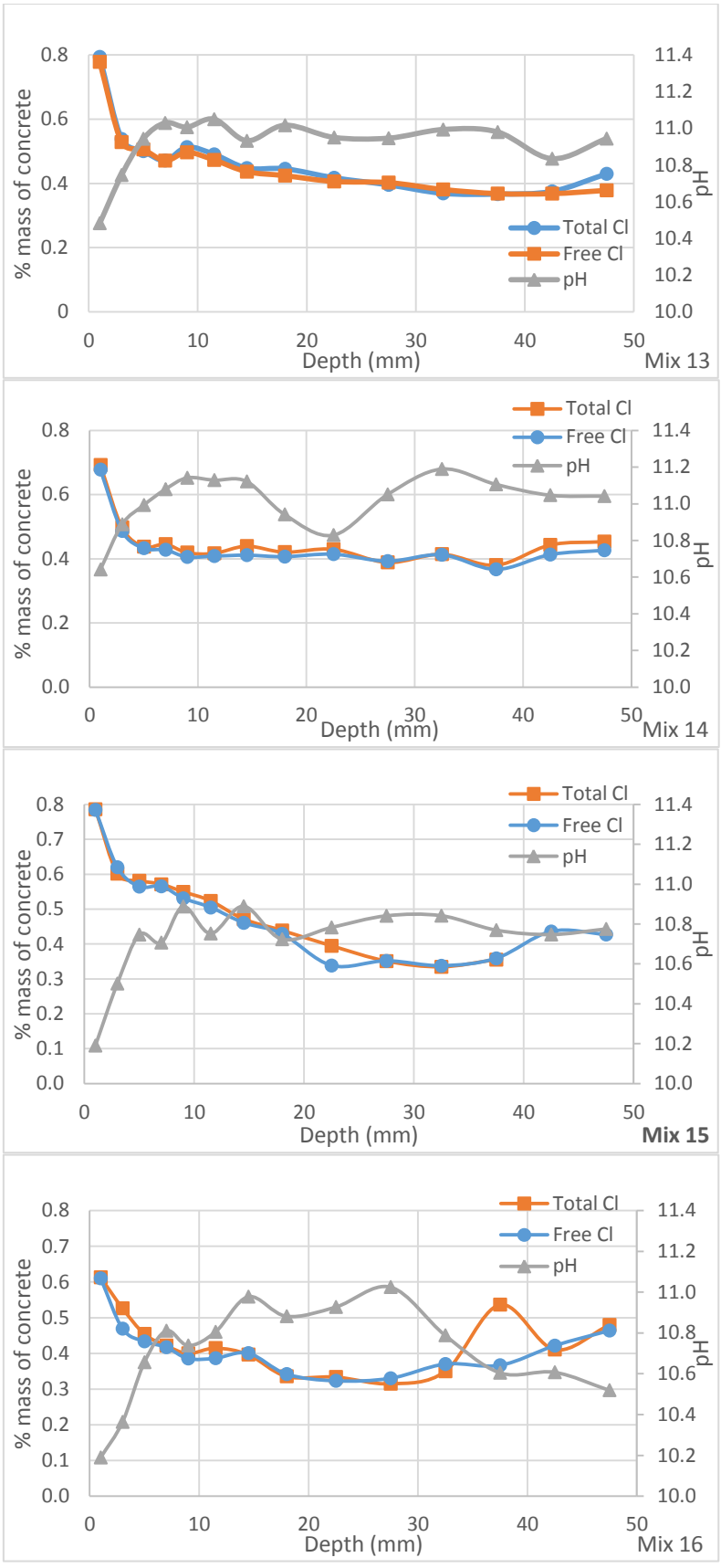

Figure 14 Total and water-soluble chloride concentration and pH for concrete dust samples collected for NT Build 443 test for mixes 13, 14, 15 and 16

Highlights

- AA-GGBS/FA concrete cured at 20^{o}C results in desirable fresh properties and strength.
- A higher proportion of GGBS results in high early and long-term strength.
- AA-GGBS/FA concretes with GGBS/FA<4 are non-viable for protection of steel in chloride environments.
- There is no chloride binding capacity in the fly ash dominated AA-GGBS/FA concretes.
- The chloride diffusivity in AA-GGBS/FA concretes depends mostly on the pore structure.

Supplementary MATLAB .fig files

Click here to download Supplementary MATLAB .fig files: Fig 3(a).fig

Supplementary MATLAB .fig files

Click here to download Supplementary MATLAB .fig files: Fig 3(b).fig

Supplementary MATLAB .fig files

Click here to download Supplementary MATLAB .fig files: Fig 5.fig

Supplementary MATLAB .fig files

Click here to download Supplementary MATLAB .fig files: Fig 7(a).fig

Supplementary MATLAB .fig files

Click here to download Supplementary MATLAB .fig files: Fig 7(b).fig

Supplementary MATLAB .fig files

Click here to download Supplementary MATLAB .fig files: Fig 7(c).fig

Supplementary MATLAB .fig files

Click here to download Supplementary MATLAB .fig files: Fig 10.fig

Supplementary MATLAB .fig files

Click here to download Supplementary MATLAB .fig files: Fig 13.fig